Available online at www.sciencedirect.com

ScienceDirect

IFAC Papers Online CONFERENCE PAPER ARCHIVE

IFAC-PapersOnLine 49-7 (2016) 400–405

Spline Fluid Models for Optimization

Esmaeil Jahanshahi, Bjarne Grimstad, Bjarne Foss

Department of Engineering Cybernetics, Norwegian University of Science and Technology, 7491 Trondheim, Norway (e-mail: bjarne.foss@ntnu.no).

Abstract: Oil production optimization is usually formulated by applying mass and momentum balances of the production network. By including temperature as a variable in pipe pressure drop, pump, and compressor models one may improve their accuracy, as well as the accuracy of the overall production system model. In addition, it is sometimes desirable to add temperature constraints to avoid flow assurance issues (*e.g.* wax and gas hydrates). The introduction of temperatures in the optimization problem requires thermodynamic properties of the fluid as functions of pressure and temperature. In this paper, a unifying fluid model for optimization using B-splines is presented. The fluid model can be constructed based on a Black-Oil model or from PVT simulations. The B-spline has properties that make it suitable for optimization. The applicability of the method is demonstrated in two examples, and the results are compared with realistic Olga simulator output.

Keywords: Energy balance, petroleum, multiphase flow, surrogate model, flow assurance

1. INTRODUCTION

Model-based approaches are increasingly used to improve the economic profit and safety of the operation in subsea oil and gas production; several testimonials to this can be found in the literature, cf. (Stenhouse, 2008; Foss, 2012).

The mass and momentum balances in the oil production network have been modeled in several works (Gunnerud and Foss, 2010; Codas and Camponogara, 2012). In the recent work by Grimstad et al. (2015a), B-spline surrogate models were used to model the nonlinear relationship between flow rates, pressure, and temperatures in multiphase pipe flow. This work did include temperature drop models, but assumed constant fluid properties. To extend this work, we propose to also model the fluid characteristics with B-splines.

In this work, we build a fluid model by fitting splines to a PVT table or black-oil model of the fluid. The splines approximate fluid properties such as the gas mass fraction and densities. The splines are nonlinear functions of the pressure and temperature that may act as surrogates for PVT simulations. When the underlying fluid model is a black-oil model, splines are used also to represent the gas compressibility factor, gas heat capacity, effective molecular weight of oil and the bubble point factor of the Lasater correlation.

An advantage with using splines is that, regardless of what the underlying fluid model is (PVT or black-oil), the resulting splines will be smooth functions with analytical derivatives readily available (Piegl and Tiller, 1997). Note that the B-spline model is nonparametric; consequently, a new B-spline must be constructed if conditions such as the oil composition were to change.

⋆ Financial support for this research was provided by Center for Integrated Operations in the Petroleum Industry (IO Center).

To display the versatility of the spline fluid models we consider two modeling applications. First, we consider the modeling of subsea manifolds (commingled flows). Our objective is to find the temperature of the outlet stream from the flow rates and the temperatures of inlet streams. For this, we use the energy balance of mixing processes based on the inflow and outflow of the enthalpy.

Next, we develop a model for the heat transfer from the three-phase petroleum fluid into the environment through the pipe walls. Since the pipe properties and ambient conditions change slowly with time, we apply a steady-state model for the heat transfer. However, calculating the heat transfer coefficients (conductive and convective) requires extensive modeling efforts; it requires the consideration of pipe geometry, insulations and ambient fluid properties. Instead, we obtain the model from input-output data where the cubic B-splines are used for this modeling.

This paper is organized as follows. The spline approximation theory is described in Section 2. Then, this theory is used to define the fluid models in Section 3. Two applications of the fluid models are presented in Sections 4 and 5 which are basis for the energy balance model. The energy balance model is tested in two case studies in Section 6. Finally, the concluding remarks are given in Section 7.

2. SPLINE SURROGATE MODELS

A surrogate model can be written as

$$\Phi(x) = \sum_{i=1}^{N} c_i \phi_i(x), \tag{1}$$

where c_i are the coefficients and ϕ_i are the basis functions. Remark that the surrogate model is *linear* wrt. the coefficients; the basis functions are in general nonlinear in $x \in \mathbb{R}^n$, making Φ a nonlinear function wrt. x. The choice

2405-8963
Peer review under responsibility of International Federation of Automatic Control.
10.1016/j.ifacol.2016.07.374

of basis functions determines the characteristics of Φ. For example, when ϕ_i are B-spline basis functions (piecewise polynomials), Φ becomes a spline function. Another class of basis functions are the radial basis functions. For such cases, Φ sometimes is referred to as a radial basis function network. An example of the latter is the *thin-plate spline*: $\phi_i(x) = ||x - x_i||_2^2 \ln(||x - x_i||_2)$, where x_i is a fixed point.

Next, consider the process of constructing of a surrogate model $\Phi : \mathbb{R}^n \to \mathbb{R}$ that approximates a (possibly unknown) function $\mathcal{F} : \mathbb{R}^n \to \mathbb{R}$.

(1) Sampling of the target function $\mathcal{F}$
(2) Fitting the surrogate model Φ to the data samples
(3) Assessing the approximation error $||\mathcal{F} - \Phi||$
    (a) If error is acceptable: stop
    (b) Otherwise: go to Step 1

An important trade-off related to this process is that of achieving a low approximation error (which may require many sample points) with few sample points (in cases where $\mathcal{F}$ is expensive to evaluate). Furthermore, if the evaluation of $\mathcal{F}$ contains random noise, care must be taken to avoid overfitting the data. A general rule of thumb – based on the principle of *Occam's razor* – is to select among models with acceptable approximation error, the one with the fewest basis functions.

Consider Step 1: Sampling of $\mathcal{F}$. We denote the set of sample points $\{x_i, y_i\}$ for $i = 1, \ldots, M$ and collect the outputs in the vector $y = [y_i]_{i=1}^M$.

In Step 2 we use the sample points to build the surrogate model. To do this, we construct the matrix $A \in \mathbb{R}^{M \times N}$ by evaluating the basis functions, so that $A_{ij} = \phi_j(x_i)$. Since the surrogate model is linear in the coefficients, the problem of fitting Φ to the data can be written as the following least-squares problem:

$$\min_c ||Ac - y||_2^2, \tag{2}$$

where the variables are the coefficients $c = [c_i]_{i=1}^N$. Assuming that we have at least as many samples as basis functions ($M \geq N$), the general solution to (2) is $c^* = (A^\mathsf{T} A)^{-1} A^\mathsf{T} y = A^\dagger y$, where $A^\dagger$ denotes the Moore–Penrose pseudoinverse.

In the special case where $M = N$, $||Ac^* - y|| = 0$ since it is possible to select the coefficients so that all sample points are interpolated. This illustrates that it is not sufficient to assess the approximation error from the value of the least-squares objective function alone. Additional sampling is required to gauge how well Φ fits the $\mathcal{F}$. This is done in Step 3 of the surrogate building process. It is also worth noting that the objective in (2) may be augmented with a regularization term to combat overfitting.

In this work we have favoured cubic B-spline basis functions, yielding a cubic B-spline surrogate model. The cubic B-spline can be constructed to obtain a high degree of smoothness – under mild assumptions it yields the interpolant in C^2 that minimizes the second-order derivative (Piegl and Tiller, 1997). Furthermore, there are fast and numerically stable algorithms for evaluating the B-spline and its derivatives, which make them suitable for optimization, as advocated by Grimstad et al. (2015a).

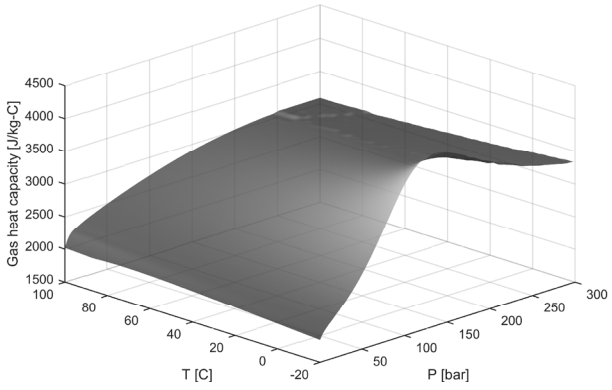

Fig. 1. Spline model for gas heat capacity, $\Phi_c^g(P, T)$

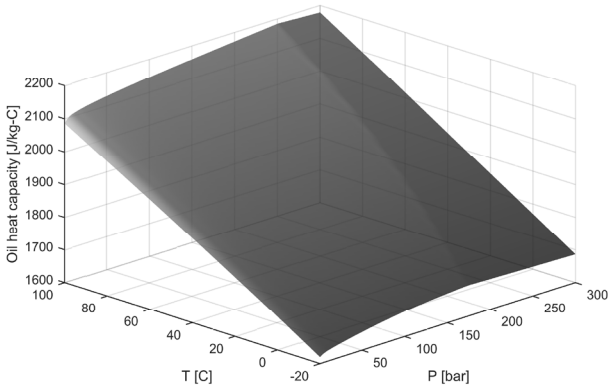

Fig. 2. Spline model for oil heat capacity, $\Phi_c^o(P, T)$

3. FLUID MODELS

Petroleum is a volatile mixture of different hydrocarbons; it expands in low pressures and light hydrocarbons (C1-C4) leave the liquid phase. Therefore, the fluid properties change for different pressures and temperatures. The gas mass fraction and other fluid properties (*e.g.* viscosity and density) at different pressures and temperature conditions can be obtained from PVT simulations or a Black Oil Model (Ahmed, 2010).

The composition of the petroleum is defined by the mole fraction or mass fraction of different light and heavy hydrocarbons, ranging from C1 to C40 or even heavier components. The composition must be known in order to perform a PVT simulation. PVTsim® is a widely used commercial package for this purpose. The results of the PVT simulation from PVTsim® are exported in tables and used as input data for flow simulators such as OLGA®. In the PVT tables, each data point corresponds to a specific pair of pressure and temperature.

In this work, we fit cubic splines to the PVT tables, following the model building process in Section 2. This yields nonlinear approximations in pressure and temperature, referred to as spline surrogate models. The fluid properties used in the proposed energy balance model are listed in Table 1. The spline models for the gas heat capacity and the oil heat capacity are shown Figures 1 and 2.

Table 1. Spline fluid models

Fluid property	Symbol	Unit	Spline Model
Gas heat capacity	$C_{\mathrm{p}}^{\mathrm{g}}$	J/(kg-C)	$\Phi_{\mathrm{c}}^{\mathrm{o}}(P,T)$
Oil heat capacity	$C_{\mathrm{p}}^{\mathrm{o}}$	J/(kg-C)	$\Phi_{\mathrm{c}}^{\mathrm{g}}(P,T)$
Water heat capacity	C_{p}^{w}	J/(kg-C)	$\Phi_{\mathrm{c}}^{\mathrm{w}}(P,T)$
Gas density	ρ^{g}	kg/m^3	$\Phi_{\rho}^{\mathrm{g}}(P,T)$
Oil density	ρ^{o}	kg/m^3	$\Phi_{\rho}^{\mathrm{o}}(P,T)$
Water density	ρ^{w}	kg/m^3	$\Phi_{\rho}^{\mathrm{w}}(P,T)$
Gas mass fraction	$\alpha_{\mathrm{m}}^{\mathrm{g}}$	kg/kg	$\Phi_{\alpha}^{\mathrm{g}}(P,T)$

4. ENERGY BALANCE OF MANIFOLDS

A manifold can be modeled as a mixing process in which different well streams are inlets and the outlet goes to a flowline. Fig. 3 shows such a process where two inlet streams and one outlet stream are shown. There is no accumulation of mass and energy in this mixing process, and no mechanical (shaft) work is done here. For simplicity, the process can be assumed adiabatic (no heat loss).

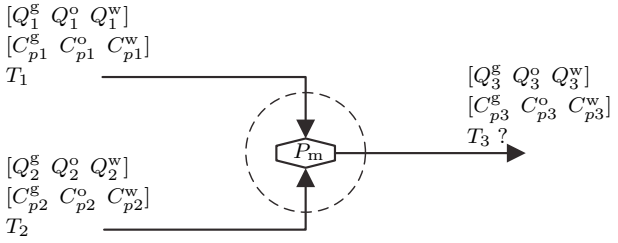

Fig. 3. Three phase mixing process

First, we formulate the energy balance when constant heat capacity is assumed. The mass balance gives

$$\dot{m}_3 = \dot{m}_1 + \dot{m}_2 \quad [\mathrm{kg/s}]$$

and the energy balance $H_{out} = H_{in}$ gives

$$H_3 = H_1 + H_2 \quad [\mathrm{J/s}]$$

where H denotes the enthalpy. No reaction takes place and we choose the three streams at T_{ref} to be at the reference state. With constant heat capacity C_p [J/kg-C], the (absolute) enthalpy is $H = \dot{m}C_{\mathrm{p}}(T - T_{ref})$.

By combining the energy balance and mass balance, the outlet temperature T_3 is expressed as

$$T_3 = \frac{\dot{m}_1 C_{\mathrm{p1}} T_1 + \dot{m}_2 C_{\mathrm{p2}} T_2}{C_{\mathrm{p3}}(\dot{m}_1 + \dot{m}_2)} + T_{ref}\left(1 - \frac{\dot{m}_1 C_{\mathrm{p1}} + \dot{m}_2 C_{\mathrm{p2}}}{C_{\mathrm{p3}}(\dot{m}_1 + \dot{m}_2)}\right). \quad (3)$$

By choosing $T_{ref} = 0^\circ$ C, the second term in (3) is omitted, and we get

$$T_3 = \frac{\dot{m}_1 C_{\mathrm{p1}} T_1 + \dot{m}_2 C_{\mathrm{p2}} T_2}{C_{\mathrm{p3}}(\dot{m}_1 + \dot{m}_2)} = \frac{H_1 + H_2}{C_{\mathrm{p3}}(\dot{m}_1 + \dot{m}_2)}. \quad (4)$$

Similarly, the outlet temperature of a general manifold with N inlet streams is calculated as follows.

$$T_j = \frac{\sum_{i=1}^{N} H_i}{C_{\mathrm{p}j}\sum_{i=1}^{N}\dot{m}_i} = \frac{\sum_{i=1}^{N}\dot{m}_i C_{\mathrm{p}i} T_i}{C_{\mathrm{p}j}\sum_{i=1}^{N}\dot{m}_i}, \quad (5)$$

where the subscript j denotes the outlet. It is not possible to calculate $C_{\mathrm{p}j}$ directly; because T_j would be needed for the spline fluid models. Instead, we use the average of $C_{\mathrm{p}i}$ weighted by mass flow rates.

$$C_{\mathrm{p}j} = \frac{\sum_{i=1}^{N}\dot{m}_i C_{\mathrm{p}i}}{\sum_{i=1}^{N}\dot{m}_i} \quad (6)$$

By combining (5) and (6) we get

$$T_j = \frac{\sum_{i=1}^{N} H_i}{\sum_{i=1}^{N}\dot{m}_i C_{\mathrm{p}i}} = \frac{\sum_{i=1}^{N}\dot{m}_i C_{\mathrm{p}i} T_i}{\sum_{i=1}^{N}\dot{m}_i C_{\mathrm{p}i}}. \quad (7)$$

Next, we consider the mixing of three phase streams. The average heat capacity of a three-phase mixture is found by averaging heat capacities of phases weighted by their mass flow rates,

$$C_{\mathrm{p}i} = \frac{\sum_{f=\{\mathrm{g,o,w}\}}\dot{m}_i^f C_{\mathrm{p}}^f}{\sum_{f=\{\mathrm{g,o,w}\}}\dot{m}_i^f} = \frac{\sum_{f=\{\mathrm{g,o,w}\}}\dot{m}_i^f \Phi_{\mathrm{c}}^f(P_i,T_i)}{\sum_{f=\{\mathrm{g,o,w}\}}\dot{m}_i^f},$$

where the superscript f denotes the phase. Assuming there is no mechanical work and choosing $T_{ref} = 0^\circ$ C, we get

$$H_i = \sum_{f=\{\mathrm{g,o,w}\}} T_i \dot{m}_i^f \Phi_{\mathrm{c}}^f(P_i,T_i). \quad [\mathrm{J/s}] \quad (8)$$

In steady-state the combined three-phase mass flow rate of each stream is the same as in the standard conditions,

$$\dot{m}_i = \rho_{\mathrm{st}}^{\mathrm{g}} Q_i^{\mathrm{g}} + \rho_{\mathrm{st}}^{\mathrm{o}} Q_i^{\mathrm{o}} + \rho_{\mathrm{st}}^{\mathrm{w}} Q_i^{\mathrm{w}}. \quad (9)$$

The water phase is incompressible and this follows

$$\dot{m}_i^{\mathrm{w}} = \rho_{\mathrm{st}}^{\mathrm{w}} Q_i^{\mathrm{w}}. \quad (10)$$

The gas and the oil mass flow rates can be obtained from the gas mass fraction α_m^g.

$$\dot{m}_i^{\mathrm{g}} = \alpha_{\mathrm{m}}^{\mathrm{g}}(\rho_{\mathrm{st}}^{\mathrm{g}} Q_i^{\mathrm{g}} + \rho_{\mathrm{st}}^{\mathrm{o}} Q_i^{\mathrm{o}}) \quad (11)$$

$$\dot{m}_i^{\mathrm{o}} = (1 - \alpha_{\mathrm{m}}^{\mathrm{g}})(\rho_{\mathrm{st}}^{\mathrm{g}} Q_i^{\mathrm{g}} + \rho_{\mathrm{st}}^{\mathrm{o}} Q_i^{\mathrm{o}}) \quad (12)$$

All densities and volumetric flow rates in (9)-(12) are given for the standard conditions. After calculating the heat capacities and the mass rates, we apply (7) to get T_j.

5. HEAT TRANSFER FROM FLOWLINES

The objective is to estimate the outlet temperature of a flowline T_{out} from the inflow boundary conditions and the outlet pressure. The temperature model is assumed to be on the form

$$\hat{T}_{\mathrm{out}} = \mathcal{F}_{\mathrm{T}}(Q_{\mathrm{in}}^{\mathrm{g}}, Q_{\mathrm{in}}^{\mathrm{o}}, Q_{\mathrm{in}}^{\mathrm{w}}, T_{\mathrm{in}}, P_{\mathrm{out}}). \quad (13)$$

In flow simulators, the inlet flow rates, the inlet temperature, and the outlet pressure are usually set as the boundary condition. These are independent variables set by the user. In the same way, these are inputs of the model in (13). The model has **five** input arguments and the modeling requires input-output data samples in five dimensions. If the data sampling grid is chosen such that there are 10 points in each dimension, we require 10^5 data samples. The experimental design, even a simulation setup, to obtain such a data-set is very time-consuming. Therefore, we aim for a model with fewer dimensions.

5.1 First principle energy balance of pipeline

Assuming no energy accumulation in the pipe and no shaft (or electrochemical) work along the pipe, the energy balance of the pipeline (Fig. 4) becomes

$$H_{\mathrm{in}} - H_{\mathrm{out}} = \dot{Q} = C_h A(T_f - T_a), \quad [\mathrm{J/s\ or\ W}] \quad (14)$$

where $\dot{Q}$ is the heat transfer rate. The cross-section area of the pipe A and the heat transfer coefficient

C_h [W/(m^2°C)] are constant values. In addition, the ambient temperature T_a is a constant which is usually equal to $4°C$ for the offshore pipelines. However, the fluid temperature T_f along the pipe is not constant and, in general, the temperature profile is not linear. Hence it is not possible to pick an average value as the T_f. The inflow enthalpy H_{in} in (14) can be calculated from (8), but it is not possible to obtain H_{out}, because the outlet temperature would be needed for $\Phi_c^f(P,T)$.

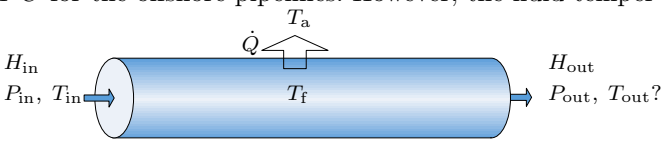

Fig. 4. Energy Balance of pipeline.

5.2 Energy balance of pipeline using splines

The inlet enthalpy in (8) contains the flow information. In other words, the effective features of the flow rates on the energy balance are encapsulated in the enthalpy. Therefore, we can remove the three flow rates from the model in (13) and instead use the enthalpy. We get the following model structure with **three** inputs.

$$\hat{T}_{out} = \Phi_T(H_{in}, T_{in}, P_{out}) \quad (15)$$

In addition to the inlet enthalpy H_{in}, the inlet temperature T_{in} is included in the model, because T_{out} has a direct and approximately linear relationship with T_{in}. Although the model is able to produce acceptable predictions without the pressure, including the pressure increases the accuracy.

In order to implement the proposed model Φ_T in (15) by a B-spline all the input arguments must be independent variables. However, the inlet enthalpy H_{in} is dependent on other variables. To generate the data set required for the modeling, we changed the inlet flow rate W_{in}, the inlet temperature T_{in} and the outlet pressure P_{out}, and we get $N_W \times N_T \times N_P$ data points.

Before using H_{in} as input data to construct the Φ_T B-spline, we perform a pre-processing on the data. For this, we generate N_P 'thin plate splines' to make N_P models for given pressure values.

$$\hat{T}^i_{out} = \Gamma^i_T(H'_{in}, T'_{in}), \quad i = 1 \dots N_P, \quad P_{out} = \mathbf{P}_{out}(i) \quad (16)$$

Here, the two the input arguments H'_{in} and T'_{in} and the output $\hat{T}^i_{out}$ have the same dimension of $N_W \times N_T$, and H'_{in} is calculated from (8). Then, we use Γ^i_T splines to generate a 3-D data set for the modeling of Φ_T.

6. EXAMPLES

6.1 Heat loss from flowline

We have simulated a horizontal pipe (Fig. 5) in the OLGA simulator. The pipeline has 10 inches diameter and 4000 meters length. We use the 'Parametric Study' functionality in the simulator to generate two data sets for the model training and validation. The inlet mass flow rate W_{in}, the inlet temperature T_{in} and the outlet pressure P_{out} are the boundary conditions of the model used for the parametric study. The boundary conditions used for the training and validation of the model are given in Table 2. To verify that the model works for different inflow conditions, we used a fixed value of 50% water-cut for the training case, and used different values of water-cut for the validations case. Although, the water cut does not appear in the model explicitly, it is included in enthalpy calculations.

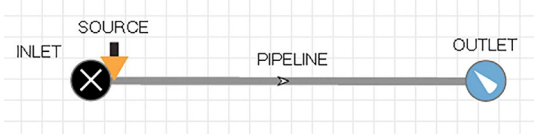

Fig. 5. Single pipeline case used in Olga simulations

Table 2. Boundary conditions of Olga model

	Training data	Validation data
WC [%]	50	10, 20, 30, 40, 50
W_{in} [kg/s]	3:3:15, 20, 25:5:70	10, 17, 22, 33, 42, 53, 63
T_{in} [°C]	15, 30, 45, 60, 75, 90	20, 40, 60, 80
P_{out} [bar]	30, 50, 70, 90, 110	20, 40, 60, 80, 100

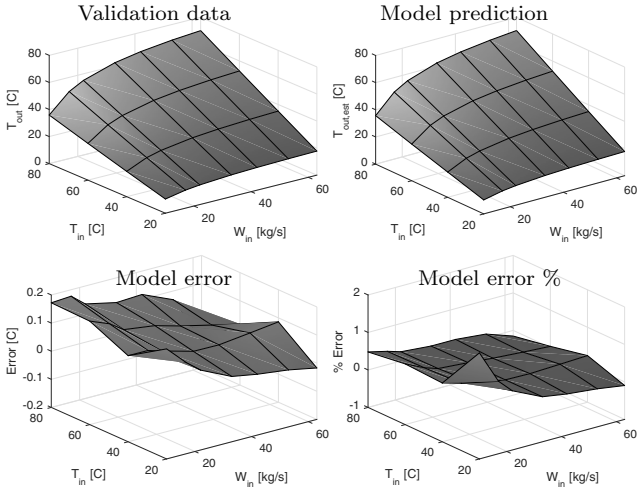

Fig. 6. Validation data for $WC = 20\%$ compared to model prediction ($\hat{T}_{out} = \Phi_T(H_{in}, T_{in}, P_{out})$)

Table 3. Maximum error [C] in model prediction for different pressures and water-cuts

	$P_{out} = 40$	$P_{out} = 60$	$P_{out} = 80$	$P_{out} = 100$
WC=10%	0.33	0.25	0.26	0.25
WC=20%	0.28	0.18	0.19	0.18
WC=30%	0.19	0.14	0.13	0.13
WC=40%	0.13	0.12	0.12	0.12
WC=50%	0.26	0.26	0.26	0.26

To create the B-spline model $\Phi_T(H_{in}, T_{in}, P_{out})$, we use the function approximation software SPLINTER (Grimstad et al., 2015b), which supports B-splines and radial basis functions in any dimension.

As mentioned earlier, we generated the model for a fixed value of 50% water-cut. Fig. 6 shows the model prediction on the validation data set where we have used 20% for the water-cut. The maximum error of the model prediction is less that 0.2 $°C$ (1% error). Table 2 shows the maximum error in the model prediction for different values of the outlet pressure and the water-cut. The accuracy of the model is acceptable also when changing the water-cut.

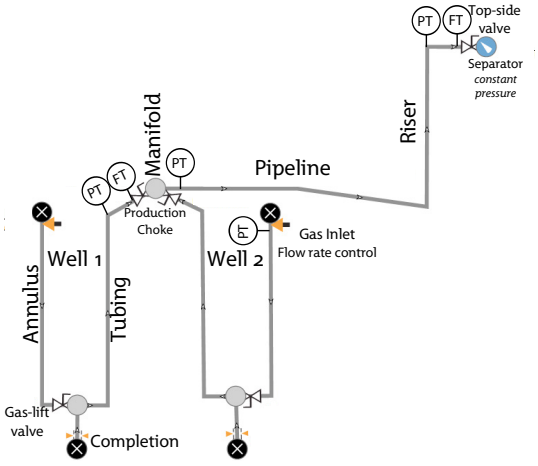

Fig. 7. OLGA-model: Oil gathering system

6.2 Gas-lift optimization with temperature constraint

Here, we consider production optimization for an oil gathering network. Fig. 7 shows the network as modeled in the Olga simulator. The network consists of two gas-lift oil wells connected to a common pipeline-riser system through a subsea manifold. The riser leads the fluid to a topside separator. The two wells have the same dimensions, but produce from separate reservoirs with different pressures and temperatures. We have $P_r = 160\,\text{bar}$ and $T_r = 90\,^\circ\text{C}$ for well 1, and $P_r = 170\,\text{bar}$ and $T_r = 115\,^\circ\text{C}$ for well 2.

The objective function aims at maximizing an economical value, based on the oil production and the gas injection at the given prices r_o and r_g. The decision variables are gas injection rates for the two wells and pressure drops of the three control valves in the system. In addition, we include the manifold pressure in the decision variables to retain five DOF, because there is an equality constraint imposed by the manifold pressure.

$$\mathbf{u} = [\dot{m}^\text{inj}_\text{w1}, \dot{m}^\text{inj}_\text{w2}, \Delta P_\text{w1}, \Delta P_\text{w2}, \Delta P_\text{top}, P_\text{m}]^T$$

The optimization problem is formulated as follows.

$$\begin{aligned} \max_{\mathbf{u}} \; & r_\text{o}(\dot{m}^\text{o}_\text{w1} + \dot{m}^\text{o}_\text{w2}) - r_\text{g}(\dot{m}^\text{inj}_\text{w1} + \dot{m}^\text{inj}_\text{w2}) \qquad (17)\\ \text{s.t.}: \; & P_\text{m} = \Phi_\text{p,m}(T_\text{m}, \alpha^\text{g}_\text{m}, \dot{m}_\text{in}, \Delta P_\text{top}),\\ & T_\text{top} > 36,\\ & \mathbf{b}^\text{u}_l \le \mathbf{u} \le \mathbf{b}^\text{u}_u, \end{aligned}$$

where P_m is the manifold pressure, and $\Phi_\text{p,m}$ is a spline model for the manifold pressure. The two wellheads are connected to the manifold, and the two wellhead pressures are given as

$$\begin{aligned} P_\text{wh1} &= P_\text{m} + \Delta P_\text{w1},\\ P_\text{wh2} &= P_\text{m} + \Delta P_\text{w2}. \end{aligned}$$

The wax deposition occurs at low temperatures (Bai and Bai, 2005). In this example, we set 36°C as the lower limit of the topside temperature T_top to prevent the wax.

First, we calculate the manifold temperature based on the mixing formula in (7).

$$H_\text{m} = T_\text{w1} \sum_{f=\text{g,o}} \dot{m}^f_\text{w1} C^f_{p,\text{w1}} + T_\text{w2} \sum_{f=\text{g,o}} \dot{m}^f_\text{w2} C^f_{p,\text{w2}}, \qquad (18)$$

$$T_\text{m} = \frac{H_\text{m}}{\sum_{f=\text{g,o}} \dot{m}^f_\text{w1} C^f_{p,\text{w1}} + \sum_{f=\text{g,o}} \dot{m}^f_\text{w2} C^f_{p,\text{w2}}}. \qquad (19)$$

Then, we apply the model proposed in (15) to calculate the topside temperature,

$$T_\text{top} = \Phi_\text{T,top}(H_\text{m}, T_\text{m}, \Delta P_\text{top}). \qquad (20)$$

The optimization model includes also the mass balance,

$$\begin{aligned} \dot{m}_\text{in} &= \dot{m}^\text{g}_\text{w1} + \dot{m}^\text{o}_\text{w1} + \dot{m}^\text{g}_\text{w2} + \dot{m}^\text{o}_\text{w2},\\ \alpha^\text{g}_\text{m} &= \frac{\dot{m}^\text{g}_\text{w1} + \dot{m}^\text{g}_\text{w2}}{\dot{m}_\text{in}}, \end{aligned}$$

where α^g_m is the gas mass fraction at the manifold, directly calculated from the mass rates. The heat capacities of the gas and liquid are described by the B-spline models.

$$\begin{aligned} C^\text{g}_p &= \Phi^\text{g}_\text{c}(P, T),\\ C^\text{o}_p &= \Phi^\text{o}_\text{c}(P, T). \end{aligned}$$

Similarly, the flow and temperature models for the two wells are also described by B-splines.

$$\begin{aligned} \dot{m}^\text{o}_\text{w1} &= \Phi_\text{o,w1}(P_\text{wh1}, \dot{m}^\text{inj}_\text{w1}),\\ \dot{m}^\text{o}_\text{w2} &= \Phi_\text{o,w2}(P_\text{wh2}, \dot{m}^\text{inj}_\text{w2}),\\ \dot{m}^\text{g}_\text{w1} &= \Phi_\text{g,w1}(P_\text{wh1}, \dot{m}^\text{inj}_\text{w1}),\\ \dot{m}^\text{g}_\text{w2} &= \Phi_\text{g,w2}(P_\text{wh2}, \dot{m}^\text{inj}_\text{w2}),\\ T_\text{w1} &= \Phi_\text{T,w1}(P_\text{wh1}, \dot{m}^\text{inj}_\text{w1}),\\ T_\text{w2} &= \Phi_\text{T,w2}(P_\text{wh2}, \dot{m}^\text{inj}_\text{w2}) \end{aligned}$$

The two gas-lift oil wells are open-loop unstable for low gas injection rates, and they are stabilized by low-level controllers. A minimum pressure drop must exist over the control valves for the controllability reason. The bound constraints for the decision variables are defined as follows.

$$\begin{aligned} \mathbf{b}^\text{u}_u &= [2.0, 2.0, 20\times10^5, 20\times10^5, 20\times10^5, 30\times10^5]^\text{T},\\ \mathbf{b}^\text{l}_u &= [0.5, 0.5, 3.0\times10^5, 3.0\times10^5, 1.5\times10^5, 15\times10^5]^\text{T}. \end{aligned}$$

To solve the optimization problem in (17), we use IPOPT (Wächter and Biegler, 2005) interfaced with Matlab. The oil price is assumed to be the normalized value of $r_\text{o} = 1$, and we consider two gas price scenarios.

Cheap gas scenario: First, we assume the normalized gas price is $r_\text{g} = 0.25$. The solver converges to this value: $[1.63, 1.64, 3.0\times10^5, 3.0\times10^5, 1.5\times10^5, 25.54\times10^5]^\text{T}$ The solution is shown in Fig. 8 where the optimal value is 31.04 indicated by the star. For demonstration purposes, we use $u_1 + u_2$ and $u_3 + u_4$ on the X and Y axis. Here, the three constraints on the pressure drop over the valves are active. The dashed line in Fig. 8 shows the sum of pressure constraints on the two wellhead valves. It is as expected that the valves are open as much as possible to increase the production rate. The topside temperature at the optimal solution is 36.89 $^\circ C$.

By a visual inspection of Figures 8, it may seem like the solver has not converged to the optimal point. However, the equality constraint related to the manifold pressure does not allow for any further increase in the objective function. This is the added limitation imposed on multi-well systems, and an accurate evaluation of the manifold pressure as a function of temperature thus becomes important. Without this equality constraint, the problem would simplify to the optimization of each well individually.

Expensive gas scenario: Here, we assume the normalized gas price is $r_\text{g} = 3$. The solver converges to this value: $[1.2199, 1.3233, 3.0\times10^5, 3.0\times10^5, 1.5\times10^5, 22.66\times10^5]^\text{T}$ The solution is shown in Fig. 9 where the optimal value is

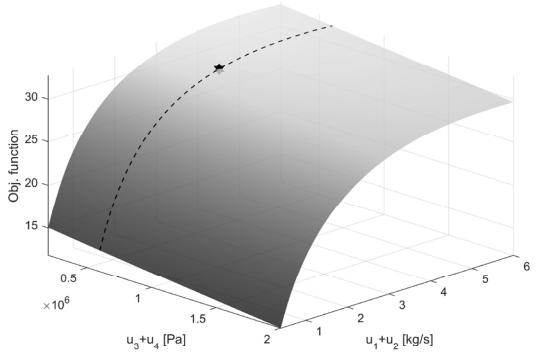

Fig. 8. Objective function for cheap gas scenario

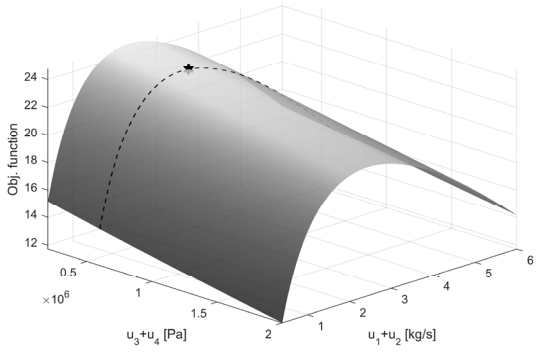

Fig. 9. Objective function for expensive gas scenario

Table 4. Comparison between optimizer prediction and Olga output

	$\dot{m}^{\mathrm{o}}_{\mathrm{w1}}$ [kg/s]	$\dot{m}^{\mathrm{o}}_{\mathrm{w2}}$[kg/s]	T_{top} °C
Olga output	14.85	16.64	35.92
Optimizer prediction	14.83	16.62	36.00

23.84. For this case, in addition to the three constraints on the pressure drop over the valves, the nonlinear inequality constraint for the topside temperature also is active, and the temperature at the solution is 36 °C.

Without the temperature inequality constraint, the solver converges to $[0.89, 0.88, 3.0\times10^5, 3.0\times10^5, 1.5\times10^5, 19.25\times10^5]^{\mathrm{T}}$, and the optimal value changes to 24.92. For the unconstrained case, the top temperature becomes 33.99 °C. However, by including the temperature constraint, the system needs to inject more gas to produce at a higher flow rate. Injecting more gas reduces the objective value, but as we saw in the temperature model, the outlet temperature increases by an increase of the inlet flow (less heat loss).

To test the accuracy of the spline models used for the optimizer, we simulated the Olga model with the optimal solution. The optimizer prediction is compared to the Olga output in Table 4. The error in flow rates is only 0.02 kg/s, and the error in the temperature is 0.08 °C.

7. CONCLUDING REMARKS

We have presented a systematic approach to model fluid properties and energy balance in an oil production network. The proposed method was tested in two examples. In the first example, the temperature model of pipeline was very accurate (99%).

The spline fluid models were successfully applied in an optimization problem including the temperature constraint. The good match between the optimizer and the Olga simulator suggests that, given an accurate temperature model, the production optimization problem can be linked with the flow assurance problem.

We showed the accuracy and other favorable numerical properties of the fluid models when described by B-splines. Thus this approach is recommended for other purposes such as in the development of flow and reservoir simulators.

ACKNOWLEDGEMENTS

Authors would like to thank Mr. Anders Wenhaug for developing the Matlab interface for SPLINTER, and for supporting us to use the software.

REFERENCES

Ahmed, T. (2010). Chapter 2 - reservoir-fluid properties. In T. Ahmed (ed.), *Reservoir Engineering Handbook (Fourth Edition)*, 29–135. Gulf Professional Publishing, Boston. doi:10.1016/B978-1-85617-803-7.50010-9.

Bai, Y. and Bai, Q. (2005). Chapter 21 - wax and asphaltenes. In Y.B. Bai (ed.), *Subsea Pipelines and Risers*, 383 – 398. Elsevier Science Ltd, Oxford. doi: 10.1016/B978-008044566-3.50023-3.

Codas, A. and Camponogara, E. (2012). Mixed-integer linear optimization for optimal lift-gas allocation with well-separator routing. *European Journal of Operational Research*, 217(1), 222–231.

Foss, B. (2012). Process control in conventional oil and gas fields - challenges and opportunities. *Control Engineering Practice*, 20(10), 1058 – 1064. doi: 10.1016/j.conengprac.2011.11.009. 4th Symposium on Advanced Control of Industrial Processes (ADCONIP).

Grimstad, B., Foss, B., Heddle, R., and Woodman, M. (2015a). Global optimization of multiphase flow networks using spline surrogate models. *Computers & Chemical Engineering*, –. doi: 10.1016/j.compchemeng.2015.08.022.

Grimstad, B. et al. (2015b). SPLINTER: a library for multivariate function approximation. `http://github.com/bgrimstad/splinter`. Accessed: 2015-09-25.

Gunnerud, V. and Foss, B. (2010). Oil production optimizationa piecewise linear model, solved with two decomposition strategies. *Computers & Chemical Engineering*, 34(11), 1803–1812.

Piegl, L.A. and Tiller, W. (1997). *The NURBS Book*. Springer Berlin Heidelberg, 2 edition. doi:10.1016/0010-4485(96)86819-9.

Stenhouse, B.J. (2008). Modelling and optimisation in bp exploration & production. In *SPE Intelligent Energy Conference and Exhibition*. Society of Petroleum Engineers, Amsterdam, The Netherlands. doi:10.2118/112148-MS. SPE-112148-MS.

Wächter, A. and Biegler, L.T. (2005). On the implementation of an interior-point filter line-search algorithm for large-scale nonlinear programming. *Mathematical Programming*, 106(1), 25–57. doi:10.1007/s10107-004-0559-y.